Supplementary file 1

Table of content

A. Building IFNγ and IL10 pathway model
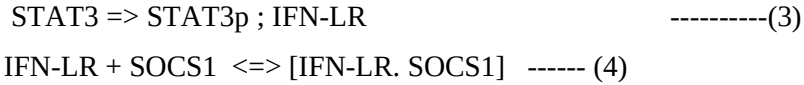
AI. Receptor activation and signaling

 IFNγ pathway

The ligand (IFNγ) binds to the receptor (IFNR) to form an active signaling complex IFN-LR. We assumed a simple activation-deactivation process in our model[1-3] which simplifies multiple biological steps of receptor signalosome formation .

$$IFNR + IFN \;\; <=> \;\; IFN\text{-}LR \qquad \text{--------- (1)}$$

The signaling complex(IFN-LR) carries out phosphorylation of STAT1 and STAT3(S/1/3). Additionally negative regulators like SOCS1[4] can bind to JAK1[5], a component embedded in the simplified IFN-LR signalosome above and subsequently inhibit the downstream signaling [1, 3, 4] .

$$STAT1 => STAT1p \; ; IFN\text{-}LR \qquad \qquad \text{--------(2)}$$

$$\text{STAT3} \Rightarrow \text{STAT3p ; IFN-LR} \qquad\qquad \text{---------(3)}$$

$$\text{IFN-LR + SOCS1} \Leftrightarrow \text{[IFN-LR. SOCS1]} \quad \text{------ (4)}$$
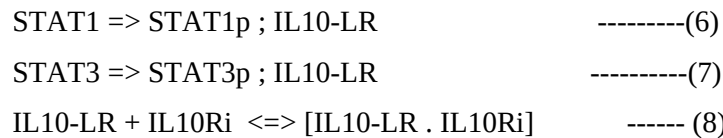
While in the reactions (2) – (3), IFN-LR acts as a modifier/enzyme, reaction (4) shows inhibition of IFN-LR by the negative regulator SOCS1. The complex [IFN-LR.SOCS1] is functionally inactive which blocks IFNγ mediated phosphorylation of S/1/3 [1].

B. IL10 pathway

Similar to the IFNγ receptor the IL10 receptor also binds to its ligand and become functionally active. In our receptor activation module explicit receptor activation deactivation steps are simplified to a one step activation and deactivation process .

$$\text{IL10R + IL10} \Leftrightarrow \text{IL10-LR} \qquad \text{--------- (5)}$$

The active signaling complex IL10-LR phosphorylates and activates STAT3 and STAT1. Stoichiometric inhibitor that typically acts by targeting the IL10R1 [5] is modeled as a potential negative regulator of IL10 signaling.

$$\text{STAT1} \Rightarrow \text{STAT1p ; IL10-LR} \qquad\qquad \text{---------(6)}$$

$$\text{STAT3} \Rightarrow \text{STAT3p ; IL10-LR} \qquad\qquad \text{---------(7)}$$

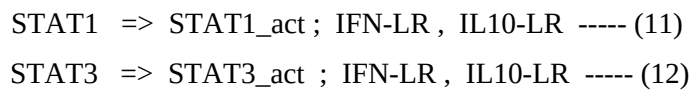$$\text{IL10-LR + IL10Ri} \Leftrightarrow \text{[IL10-LR . IL10Ri]} \qquad \text{------ (8)}$$

As observed[5], IL10Ri production and degradation is considered as a constitutive process that is independent of IL10 stimulation which are represented as the reactions below

$$\Rightarrow \text{IL10Ri} \qquad\qquad \text{--------- (9)}$$

$$\text{IL10Ri} \Rightarrow \qquad\qquad\qquad \text{--------- (10)}$$

Where reaction (9) and (10) depicts the basal production and degradation of IL10Ri.

II. STAT1 and STAT3 signaling

STAT1 and STAT3 are activated during both IFNγ and IL10 stimulations.

$$\text{STAT1} \Rightarrow \text{STAT1\_act ; IFN-LR , IL10-LR ----- (11)}$$

$$\text{STAT3} \Rightarrow \text{STAT3\_act ; IFN-LR , IL10-LR ----- (12)}$$

Studies show STAT1 and STAT3 compete with each other for the same receptor phosphotyrosine motif during IFNγ signaling [7] which is implemented in our model as a competition between both the STATs to get phosphorylated by the IFNLR. In the same lines, we implemented competition of STAT1 and STAT3 for access to IL10.

STAT1_act and STAT3_act are the activated/phosphorylated forms of STATs which subsequently undergo dimerization and become transcriptionally active[1]

$$STAT1\_act + STAT1\_act \ -> STAT1\_act\_Dm \ ----- (13)$$
$$STAT3\_act + STAT3\_act \ -> STAT3\_act\_Dm \ ----- (14)$$
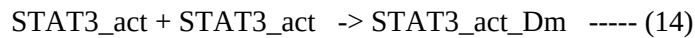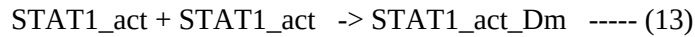
III. Transcriptional induction of SOCS1 and SOCS3

Transcriptional induction of SOCS1 and SOCS3 were experimentally measured for both IFNγ and IL10 signaling. Both the SOCS are induced relatively strongly upon IL10 signaling compared to IFNγ signaling (Figure 2B and 2D), especially SOCS1 induced upon 1L10 signaling is ~3 fold higher compared to IFNγ signaling.

In our model, in the absence of external signal basal production and degradation of the SOCS is given as

$$=> \ SOCS1 \ ----- (15)$$
$$=> \ SOCS3 \ ----- (16)$$
$$SOCS1 => \ ----- (17)$$
$$SOCS3 => \ ----- (18)$$
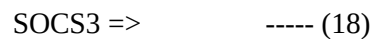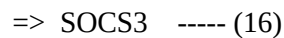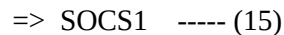
Where reaction (15)&(16) represents production and reaction (17) & (18) represents degradation of the SOCS.

Studies show upon IFNγ and IL10 signaling both the SOCS are transcriptionally induced as a function of canonical STAT1 (in IFNγ pathway) or STAT3(in IL10 pathway). In STAT1 null mice SOCS3 but not SOCS1 is induced and in STAT3 null mice SOCS3 induction is blocked [7]; thus we modeled SOCS1 and SOCS3 induction as functions STAT1 dimer(STAT1 _act_Dm) and STAT3 dimer (STAT3_act_Dm) respectively. Additionally, studies show efficient promoter binding and gene expression by STAT1 and STAT3 also depends on other complex factors like availability of other cofactors, for instance, during IFNγ stimulation, occupation of DNA-binding sites for STAT1 and the transcriptional activator Sp1 are both required for full activation of certain genes [8]. Similarly gene expression in IL10 pathway are

dependent on sp1 and sp3 cofactors [9]. Also competition of bind to different cofactors emerge between STAT1 and STAT3 [10]. Considering the complexity of such interactions and to accommodate the plausible differences in STAT1(STAT3) mediated induction of SOCS1(SOCS3) in IFNγ and IL10 pathways we assumed differences in their induction rates, Km values and hill coefficients and estimated these values during model calibration.

B. Model details

BI. Equations

The differential equations below captures the information propagation in both IFNγ and IL10 pathways. The xs' are model species and the ps are model parameters, names of the species and parameter as well as their best fit values are detailed in supplementary table TS1.

$$\frac{d[x1]}{dt} = \text{x3*p2 - x1*x2*p1 * p0}$$

$$\frac{d[x2]}{dt} = \text{x3*p2 - x1*x2*p1}$$

$$\frac{d[x3]}{dt} = \text{x1*x2*p1 - x3*p2 + x4*p4 + x4*p16 - x3*x9*p3}$$

$$\frac{d[x4]}{dt} = \text{x3*x9*p3 - x4*p16 - x4*p5 - x4*p4}$$

$$\frac{d[x5]}{dt} = \text{p8*x6*p7g + p8*x11*p7g - (x3*x5*p6)/(p9*(x5/p9 + x7/p10 + 1)) - (x15*p21*x5*p26)/(p28*(x5/p28 + x7/p29 + 1))}$$

$$\frac{d[x6]}{dt} = \text{p8*x11*p7g - p8*x6*p7g - 2*x6\^2*p11 + (x3*x5*p6)/(p9*(x5/p9 + x7/p10 + 1)) + }$$
(x15*p21*x5*p26)/(p28*(x5/p28 + x7/p29 + 1))

$$\frac{d[x7]}{dt} = \text{p8*x8*p14g + p8*x12*p14g - (x3*x7*p13)/(p10*(x5/p9 + x7/p10 + 1)) - (x15*p21*x7*p27)/(p29*(x5/p28 + x7/p29 + 1))}$$

$$\frac{d[x8]}{dt} = \text{p8*x12*p14g - p8*x8*p14g - 2*x8\^2*p12 + (x3*x7*p13)/(p10*(x5/p9 + x7/p10 + 1)) + }$$
(x15*p21*x7*p27)/(p29*(x5/p28 + x7/p29 + 1))

$$\frac{d[x9]}{dt} = \text{p15 - x9*p16 + x4*p4 + x4*p5 - x3*x9*p3 + (p19*p15*(x11/p30)\textasciicircum n2)/((x11/p30)\textasciicircum n2 + 1) +}$$
(p21*p34*p15*(x11/p32)^n1)/((x11/p32)^n1 + 1)

$$\frac{d[x10]}{dt} = \text{p17 - x10*p18 + (p20*p17*(x12/p31)\textasciicircum n22)/((x12/p31)\textasciicircum n22 + 1) +}$$
(p21*p35*p17*(x12/p33)^n11)/((x12/p33)^n11 + 1)

$$\frac{d[x11]}{dt} = \text{x6\textasciicircum 2*p11 - p8*x11*p7}$$

$$\frac{d[x12]}{dt} = \text{x8\textasciicircum 2*p12 - p8*x12*p14}$$

$$\frac{d[x13]}{dt} = \text{x15*p21*p23 - x13*x14*p21*p22}$$

$$\frac{d[x14]}{dt} = \text{x15*p21*p23 - x13*x14*p21*p22}$$

$$\frac{d[x15]}{dt} = \text{p21*x16*p25 - x15*p21*p23 + p21*x16*p37 - x15*x17*p21*p24 + x13*x14*p21*p22}$$

$$\frac{d[x16]}{dt} = \text{x15*x17*p21*p24 - p21*x16*p25 - p21*x16*p37 - p21*x16*p38}$$

$$\frac{d[x17]}{dt} = \text{p21*p36 + p21*x16*p38 - x17*p21*p37 + p21*x16*p25 - x15*x17*p21*p24}$$

The model above is calibrated to the experimental data (Figure 2), and the calibrated model is used for making predictions that were validated experimentally(Figure 3). Details of model calibration and validation steps can be found in the sections below.

BII. Species

Species	Name in model	Biological meaning
x1	IFNγ	IFNγ ligand
x2	IFNR	IFNγ receptor
x3	IFN-LR	Active signaling complex ; IFNγ pathway
x4	IFN-LR.SOCS1	Functionally inactive signaling complex
x5	STAT1	Inactive STAT1
x6	STAT1_act	Active STAT1
x7	STAT3	Inactive STAT3
x8	STAT3_act	Active STAT3
x9	SOCS1	Free SOCS1

x10	SOCS3	Free SOCS3
x11	STAT1_act_Dm	Active STAT1 dimer
x12	STAT3_act_Dm	Active STAT3 dimer
x13	IL-10	IL-10 ligand
x14	IL-10R	IL-10 receptor
x15	IL10-LR	Active signaling complex; IL-10 pathway
x16	IL10-LR.IL10Ri	Functionally inactive signaling complex
x17	IL10Ri	Inhibitor of IL10R

BII. Parameters

Parameters	Name in model
p0	IFNγ_On
p1	kf_Active_Rec_IFNγ
p2	kb_Active_Rec_IFNγ
p3	kf_feedback_IFNγ
p4	kb_feedback_IFNγ
p5	kdeg_Active_Rec_IFNγ
p6	kphos_STAT1_IFN
p7	kdephos_STAT1_IFNγ
p8	Phosphatase
p9	Km_STAT1_phos_IFN
p10	Km_STAT3_phos_IFN
p11	kDm_STAT1
p12	kDm_STAT3
p13	kphos_STAT3_IFNγ
p14	kdephos_STAT3_IFNγ
p15	kprod_SOCS1
p16	kdeg_SOCS1
p17	kprod_SOCS3
p18	kdeg_SOCS3
p19	index_k_STAT1_induced_prod_SOCS1
p20	index_k_STAT1_induced_prod_SOCS3
p21	IL10_on
p22	kf_Active_Rec_IL10
p23	kb_Active_Rec_IL10
p24	kf_feedback_IL10
p25	kb_feedback_IL10
p26	kphos_STAT1_IL10
p27	kphos_STAT3_IL10
p28	Km_STAT1_phos_IL10
p29	Km_STAT3_phos_IL10
p30	Km_STAT1_SOCS1

p31	Km_STAT1_SOCS3
p32	Km_STAT3_SOCS1
p33	Km_STAT3_SOCS3
p34	index_k_STAT3_induced_prod_SOCS1
p35	index_k_STAT3_induced_prod_SOCS3
p36	kprod_Feedback_inhibitor
p37	kdeg_Feedback_inhibitor
p38	Induced_deg_IL10_receptor
p39	n1
p40	n11
p41	n2
p42	n22

C. Model calibration and validation

To estimate the variables in the model that best explains the experimental data we fitted the dynamics of S/1/3 trajectories to the corresponding experimental measurements. We have used 16 independent experimental measurements for model calibration and three independent measurements were used to validate model predictions. As both IFNγ and IL10 pathways were built within one single model we selectively activated either of the pathways for a given stimulus condition while fitting the pathways specific experimental conditions. Only during the costimulation predictions both pathways were activated simultaneously. The calibration datasets are listed below

CI. Datasets for IFNγ pathway calibration

1. STAT1 phosphorylation kinetics at low dose(L)

2. STAT1 phosphorylation kinetics at medium dose(M)

3. STAT1 phosphorylation kinetics at high dose(H)

4. STAT3 phosphorylation kinetics at L

5. STAT3 phosphorylation kinetics at M

6. STAT3 phosphorylation kinetics at H

7. SOCS1 induction kinetics at M

8. SOCS3 induction kinetics at M

CII. Datasets for IL10 pathway calibration

1. STAT1 phosphorylation kinetics at low dose(L)

2. STAT1 phosphorylation kinetics at medium dose(M)

3. STAT1 phosphorylation kinetics at high dose(H)

4. STAT3 phosphorylation kinetics at L

5. STAT3 phosphorylation kinetics at M

6. STAT3 phosphorylation kinetics at H

7. SOCS1 induction kinetics at M

8. SOCS3 induction kinetics at M

CII. Optimization

Observables: Optimization process involved fitting observables from the model which we fitted against the experimental data. The following observables were subjected to fitting

$$\text{STAT1\_phos} = \frac{(x6+2*x11)}{(x5+x6+2*x11)} \quad \text{-------- (1)}$$

$$\text{STAT3\_phos} = \frac{(x8+2*x12)}{(x7+x8+2*x12)} \quad \text{-------- (2)}$$

$$\text{SOCS1}_{\text{IFN}\gamma} = \frac{(x4+x9)}{x9[basal]} \quad \text{-------- (3)}$$

$$\text{SOCS1}_{\text{IL10}} = \frac{x9}{x9[basal]} \quad \text{-------- (4)}$$

$$\text{SOCS3} = \frac{x10}{x10[basal]} \quad \text{-------- (5)}$$

The observables STAT1_phos and STAT3_phos captures the dynamics of phosphorylated STAT1 and STAT3, respectively. Similarly the observables SOCS1 and SOCS3 compares the fold change of induction over the basal The best fit parameters with their upper and lower bound are shown in supplementary table TS1.

Offsets and scaling factors**: During model calibration we introduced offset and scaling factors which facilitates quantitative comparison of model and data by adjusting the model trajectories without influencing the biologically significant observables and general conclusions offered by the model [11, 12]. To consider the contribution of uncertainties in experimental measurement process and additional unknown smaller technical

fluctuations on the day of the experiment we have implemented local scaling factors. In our model the optimization process minimizes the differences between the model and the data from 16 datasets simultaneously to estimate the goodness of fit (χ^2)

$$\chi^2 = \frac{\left(offset_{global} + scale_{global} * scale_{local} * model - data\right)\square^2}{error^{\square 2 \square \square}} \quad \text{----(6)}$$

Optimization was carried out using the MATLAB optimization toolbox Data2Dynamics [13] where goodness of fit (function (6)) is calculated by evaluating a log likelihood function that minimizes the difference between model and data, as well as the contribution from the fitted error models from different data sets. Details of fitting processes can be found elsewhere [13, 14]. Fitting was done using a multi-start local optimization strategy where the starting parameter vectors were generated using Latin hypercube sampling method and MATLAB function lsqnonlin was used for optimization [13, 10]. We estimated one offset_global and one scale_global for all the experimental conditions across the doses or stimulus type applied. For example, one offset_global for STAT1phos is calculated for L,M, H doses of both IFNγ and IL10 treatments. Similarly one scale_global is calculated and in each independent dataset (L, M or H) a scale_localis calculated(in the range 0.7-1.5) to accommodate plausible measurement fluctuations local to individual datasets; this also ensures that overfitting plausibly arising due to scaling factors across all datasets is minimized. The bestfit model had 321 data points(N) and χ^2 = 307.223 (N/χ^2 < 1). The model has 68 free parameters which comprises both biologically relevant model variables, indexes, offsets and scaling factors.

S1.5. Model validation

Using the best fit parameters (supplementary table TS1) we simulated the costimulation experiment where M dose of IFNγ and IL10 are applied simultaneously and the resultant dynamics of STAT1 and STAT3 activation were studied. Due to the inherent parameter uncertainties associated with such biochemical models robust predictions are often not derivable from only one best fit model [11]. So, here we used 40 independently fitted models, each with comparable goodness of fit, to predict the effect of the costimulation on STAT1 and STAT3 dynamics. We achieved quantitative agreements with data for STAT3 and SOCS1 data (Figure 4B and 4D) and STAT1 predictions(Figure S2A) could be quantitatively matched to the data(Figure 4C) by multiplying the predicted STAT1 trajectory to a scaling factor that adjusts the height of the predicted trajectory without further adjustments to the model. Shaded area in Figure 4B, 4C and 4D shows prediction range and the solid lines show the predictions from the fit with lowest χ^2 .

D. Parameter sampling

To understand the significance of individual best-fitted parameters on the signaling dynamics of the STATs we sampled the best fit parameters, simulated the model and captured the trajectories of S/1/3.

For a given variable p, varied in the range [lu*p,ub*p] where lb and ub are upper and lower bound of sampling, the following Monte-Carlo sampling method [15] was used

$$sampled\_p = (ub*p - lu*p).* random(1) + lu*p \qquad ----- (7)$$

random(1) generates a random number between 0 to 1. The method was repeated for all the sampled variables and it results in a new parameter vector. We generated 20000 such independent parameter vectors and simulated the model for each parameter vector and analyzed the STATs trajectories. The range of variation allowed for each parameter was a 5 fold in either direction, implying, ub = 5 and lb = 0.2.

E. Information content calculation

As implicated in earlier studies[15, 16], we argued, the parameters with maximum information for a desired response type would be the most sensitive parameters and they will be constrained to values in a certain range compared to the less sensitive paramters who in a much wider range can give the response of interest. For instance, if we have 2000 independent parameter sets that results in bell shaped STAT3 responses($Para_{Bell-shaped}$) to the increasing dose of IFNγ, and 2000 other independent parameter sets resulting in proportional STAT3 dose-responses ($Para_{proportional}$), then to calculate the information content of a given parameter m we first calculated the entropy of m in both $Para_{Bell-shaped}$ and $Para_{proportional}$.

$$E_{m[Bell-shaped]} \quad ¿ -\sum_{\square}^{\square} p(m) log p(m) ---- [8]$$

where p(m) implies the probability of m to be located in a given bin within the distribution it assumes in the assigned range.

Similarly, $E_{m[proportional]}$ is calculated for the parameter m. The information content of the parameter m is then calculated as[15]

$$I(m) = |E_{m[Bell-shaped]} - E_{m[proportional]}| \quad ----- [9]$$

Information content of all the model variables were calculated in a similar manner. This method was also used to calculate the information content and identify the most sensitive parameter(s) determining the robustness of IL10-STAT3 signaling during costimulation.

References

1. Yamada S, Shiono S, Joo A, Yoshimura A.Control mechanism of JAK/STAT signal transduction pathway. FEBS Lett. 2003;534: 190-196. doi:

2. Gambin A, Charzyńska A, Miklaszewska AE, Rybiński M. Computational models of the JAK1/2-STAT1 signaling. JAKSTAT. 2013;2: e24672. doi:10.4161/jkst.24672.

3. Rateitschak K, Karger A, Fitzner B, Lange F, Wolkenhauer O, Jaster R. Mathematical modelling of interferon-gamma signaling in pancreatic stellate cells reflects and predicts the dynamics of STAT1 pathway activity. Cell Signal. 2010;22: 97-105.

4. Zi Z, Cho KH, Sung MH, Xia X, Zheng J, Sun Z. In silico identification of the key components and steps in IFN-gamma induced JAK-STAT signaling pathway. FEBS Lett. 2005;579 :1101-1108. doi:10.1016/j.febslet.2005.01.009.

5. Jiang H, Lu Y, Yuan L, Liu J. Regulation of interleukin-10 receptor ubiquitination and stability by beta-TrCP-containing ubiquitin E3 ligase. PLoS One. 2011;6 :e27464. doi: 10.1371/journal.pone.0027464.

6. Gaspers LD, Bartlett PJ, Politi A, Burnett P, Metzger W, Johnston J, Joseph SK, Höfer T, Thomas AP. Cell Rep. 2014;9(4):1209-18. Hormone-induced calcium oscillations depend on cross-coupling with inositol 1,4,5-trisphosphate oscillations.

7. Qing Y, Stark GR. Alternative activation of STAT1 and STAT3 in response to interferon-gamma. J Biol Chem. 2004;279 :41679-41685.

8. Look DC, Pelletier MR, Tidwell RM, Roswit WT, Holtzman MJ. Stat1 depends on transcriptional synergy with Sp1. J Biol Chem. 1995; 270(51):30264-7.

9. Tone M, Powell MJ, Tone Y, Thompson SA, Waldmann H. IL-10 gene expression is controlled by the transcription factors Sp1 and Sp3. J Immunol. 2000;165(1):286-91.

10. Hu X, Ivashkiv LB. Cross-regulation of signaling pathways by interferon-gamma: implications for immune responses and autoimmune diseases. Immunity. 2009;;31(4):539-50.

11. Strasen J, Sarma U, Jentsch M, Bohn S, Sheng C, Horbelt D, et al.Cell-specific responses to the cytokine TGFβ are determined by variability in protein levels. Mol Syst Biol. 2018;14: e7733. doi: 10.15252/msb.20177733.

12. Bachmann J, Raue A, Schilling M, Böhm ME, Kreutz C, Kaschek D, et al. Division of labor by dual feedback regulators controls JAK2/STAT5 signaling over broad ligand range. Mol Syst Biol. 2011;7 :516. doi: 10.1038/msb.2011.50.

13. Raue A, Steiert B, Schelker M, Kreutz C, Maiwald T, Hass H, et al.Data2Dynamics: a modeling environment tailored to parameter estimation in dynamical systems. Bioinformatics. 2015 ;31(21):3558-60.

14. Raue A, Schilling M, Bachmann J, Matteson A, Schelker M, Kaschek D, et al. Lessons learned from quantitative dynamical modeling in systems biology. PLoS One. 2013; 8 :e74335.

15. Ghosh B, Sarma U, Sourjik V, Legewie S. Sharing of Phosphatases Promotes Response Plasticity in Phosphorylation Cascades. Biophys J. 2018;114(1):223-236.

16. François P., Siggia E.D. Predicting embryonic patterning using mutual entropy fitness and in silico evolution. Development. 2010;137:2385–2395.